Negative thermal expansion and magnetocaloric effect in Mn-Co-Ge-In thin films

Y. Liu, K. M. Qiao, S. L. Zuo, H. R. Zhang, H. Kuang, J. Wang, F. X. Hu, J. R. Sun, and B. G. Shen

Citation: Appl. Phys. Lett. **112**, 012401 (2018); doi: 10.1063/1.5009985
View online: https://doi.org/10.1063/1.5009985
View Table of Contents: http://aip.scitation.org/toc/apl/112/1
Published by the American Institute of Physics

Negative thermal expansion and magnetocaloric effect in Mn-Co-Ge-In thin films

Y. Liu,[1,2] K. M. Qiao,[1,2] S. L. Zuo,[1,2] H. R. Zhang,[1,2] H. Kuang,[1,2] J. Wang,[1,2,a)] F. X. Hu,[1,2,a)] J. R. Sun,[1,2] and B. G. Shen[1,2]
[1]*Beijing National Laboratory for Condensed Matter Physics and State Key Laboratory of Magnetism, Institute of Physics, Chinese Academy of Sciences, Beijing 100190, People's Republic of China*
[2]*School of Physical Sciences, University of Chinese Academy of Sciences, Beijing 100190, People's Republic of China*

(Received 21 October 2017; accepted 11 December 2017; published online 3 January 2018)

MnCoGe-based alloys with magnetostructural transition show giant negative thermal expansion (NTE) behavior and magnetocaloric effects (MCEs) and thus have attracted a lot of attention. However, the drawback of bad mechanical behavior in these alloys obstructs their practical applications. Here, we report the growth of Mn-Co-Ge-In films with thickness of about 45 nm on (001)-$LaAlO_3$, (001)-$SrTiO_3$, and (001)-Al_2O_3 substrates. The films grown completely overcome the breakable nature of the alloy and promote its multifunctional applications. The deposited films have a textured structure and retain first-order magnetostructural transition. NTE and MCE behaviors associated with the magnetostructural transition have been studied. The films exhibit a completely repeatable NTE around room temperature. NTE coefficient α can be continuously tuned from the ultra-low expansion ($\alpha \sim -2.0 \times 10^{-7}$/K) to $\alpha \sim -6.56 \times 10^{-6}$/K, depending on the growth and particle size of the films on different substrates. Moreover, the films exhibit magnetic entropy changes comparable to the well-known metamagnetic films. All these demonstrate potential multifunctional applications of the present films. *Published by AIP Publishing.*
https://doi.org/10.1063/1.5009985

MM'X alloys (M, M': transition element; X: main group element) with a Ni_2In-type hexagonal structure have received much attention for their giant magnetocaloric/barocaloric effect (MCE),[1,2] giant negative thermal expansion (NTE) behavior,[3] and magnetic field induced shape memory effect.[4] As one member of the family, the stoichiometric MnCoGe has the parent phase of Ni_2In-type hexagonal. It goes through a martensitic structural transition to the TiNiSi-type orthorhombic structure at around 420 K.[5] The ground states of the two respective structures are ferromagnetic (FM), and the intrinsic FM ordering temperatures are 355 K and 265 K for the martensitic orthorhombic and austenitic hexagonal phases,[5] respectively. The martensitic transition temperature is very sensitive to the valence electron concentration, local chemical environment, and extrinsic field such as pressure. By optimizing the composition of the alloy through introducing vacancies, interstitial elements, or replacing the main elements by atoms with different sizes and valence electrons, the martensitic transition temperature can be tuned to reside in the temperature gap of FM ordering temperature of the two respective structures. Hence, a coupling of magnetic and structural transitions, i.e., magnetostructural transition (M_s), can be induced.[5–11] The M_s transformation is accompanied by the giant barocaloric effect[2] and magnetocaloric (MCE) effect.[1] Moreover, an abnormal negative volume change of −3.9% occurs for the bulk[4] during the transition, based on which giant NTE with a coefficient as much as $\alpha \sim -51.5 \times 10^{-6}$/K in a temperature window has been obtained in the bonded Mn-Co-Ge alloys.[3] Materials with zero thermal expansion (ZTE) or precisely tailored thermal expansion are in urgent demand of modern industries. Although a number of ZTE or NTE materials as compensators have been discovered, such as ZrW_2O_8 family,[12] CuO nanoparticles,[13] $PbTiO_3$-based compounds,[14] antiperovskite manganese nitrides,[15,16] $La(Fe,Co,Si)_{13}$,[17] and MnCoGe-based compounds,[4] approaching to precisely tailored thermal expansion, particularly for ZTE, still remains a great challenge.

It is known that fabricating magnetic materials in lower dimensions can stimulate interesting properties and overcome some weakness of the bulk. In recent years, more and more work has emerged on the fabrication of thin films with magnetostructural coupling to realize textured or single crystalline structures, thus promoting their multifunctional application.[18] The thin films also facilitate the miniaturization of magnetic refrigerants, which have priorities for promoting thermal exchange of the material due to the large surface area. Many representative MCE materials such as Gd,[19] $Gd_5Si_2Ge_2$,[20,21] FeRh,[22] metamagnetic NiMn-based Heusler alloy,[23–25] and MnAs[26] have been explored in nanostructured thin films, and considerable MCE has been reported. MnCoGe-based alloys, however, have not been explored up to now. In practice, MnCoGe-based alloys with magnetostructural transition have serious weakness, that is, they will collapse into powders soon after annealing. This fact limits their application. Considering the excellent behavior of the MnCoGe-based alloys, it is worthwhile to explore the growth technique of the alloy films. Fabricating MnCoGe-based alloy films and realizing M_s in the thin films is a good way to overcome the weakness of the alloy, thus promoting their

a)Authors to whom correspondence should be addressed: fxhu@iphy.ac.cn and wangjing@iphy.ac.cn

possible application as solid-state magnetic refrigerants and NTE use as thermal compensators.

Our previous work has shown that through replacing Ge by a few In atoms, the structural transition of the alloy can be tuned to be around room temperature. M_s transformation can thus be realized in Mn-Co-Ge-In alloys.[2] Here, choosing the $MnCoGe_{0.995}In_{0.005}$ alloy as the target, we report the growth of Mn-Co-Ge-In thin films on different substrates. Analysis of the magnetic and structural transformation along with the MCE and NTE of the films grown has been done.

Films with a thickness of 45 nm were deposited on (001)-$LaAlO_3$ (LAO), (001)-$SrTiO_3$ (STO), and (001)-Al_2O_3 substrates using the pulsed laser deposition (PLD) technique. The base pressure is better than 10^{-8} mbar. The target was cold-pressed from the arc-melted $MnCoGe_{0.995}In_{0.005}$ alloy powders under pressure as high as 6 GPa.[10] The substrate temperature was kept at 823 K during deposition. The structure of the films was determined by X-ray diffraction (XRD) using Cu-Kα radiation. The morphology of the film was examined by atomic force microscopy (AFM), scanning electron microscopy (SEM), and transmission electron microscopy (TEM) techniques. Magnetization properties were measured using a Quantum Design Superconducting Quantum interference device (SQUID) VSM.

The surface morphology and microstructure of the thin films are shown in Fig. 1. It can be confirmed from the SEM images that the films are fine grained polycrystalline with a minimum size of several hundreds of nanometers. The three-dimensional image of the specific film on the LAO substrate suggests a three-dimensional (Volmer-Weber) growth mode. The high resolution TEM image of the typical film on STO denotes grain boundaries as shown in Fig. 1(d), meaning that the areas with a minimum size resolved in the SEM image are not grains but islands constituted with grains whose sizes are several tens of nanometers. The white area in the TEM image is the small island that fills in the bigger ones which correspond to the black areas of the SEM image, as shown in Fig. 1(b). The size of the islands is different for thin films grown on Al_2O_3, STO, and LAO substrates, with average values of about 1 μm, 0.66 μm, and, 0.28 μm, respectively. From the thermodynamic point of view, the growth mode of films can be analyzed from the surface free energy of the metal (γ_{metal}), oxide substrate (γ_{oxides}), and metal-oxide interface ($\gamma_{interface}$). When $\gamma_{metal+}\gamma_{interface} > \gamma_{oxides}$, the three-dimensional growth mode is supported.[27] Since γ_{metal} is usually higher than γ_{oxides},[27] the growth of the three-dimensional mode is very likely. The kinetic process is related to coalescence of islands and the incoming atoms filling the vacant spaces between the islands. This fact results in the observed morphology of the films with little islands filling between the bigger ones. Moreover, the practical growth process of metal films on the oxide substrate is complicated and closely related to the following factors, such as the free surface energy of the respective alloy film and oxide substrates, the energy barrier of the incoming metal atoms in diffusing across the surface of the oxide substrates and the film of metal islands, as well as the defect intensity of the oxide substrates. These factors finally lead to different morphologies and island sizes of the present films.

Room temperature XRD patterns of the thin films on different substrates are displayed in Fig. 2. Interestingly, the diffraction patterns denote mainly the peaks of the (00l) plane for the hexagonal structure and the (h00) plane for the orthorhombic structure. This implies that the films own mixed structures and are possibly textured along the out-of-plane direction with (001) orientation for the hexagonal structure and (h00) orientations for the orthorhombic structure. The orthorhombic structure could be formed through a diffusionless martensitic transformation and would certainly experience a huge stress as the films were cooled from the deposition temperature of 823 K. The lattice constants of the hexagonal and orthorhombic structures have the relationship of $a_O = c_H$, $b_O = a_H$, and $c_O = \sqrt{3}\ a_H$.[2,28] The c axis of the hexagonal structure corresponds to the a axis of the orthorhombic structure, which is the main deformation axis and changes by 11.3% during the martensitic transformation.[2,28] Thus, the textured structure of the films can be reasonable, with c_H and a_O axes of the two respective structures lying

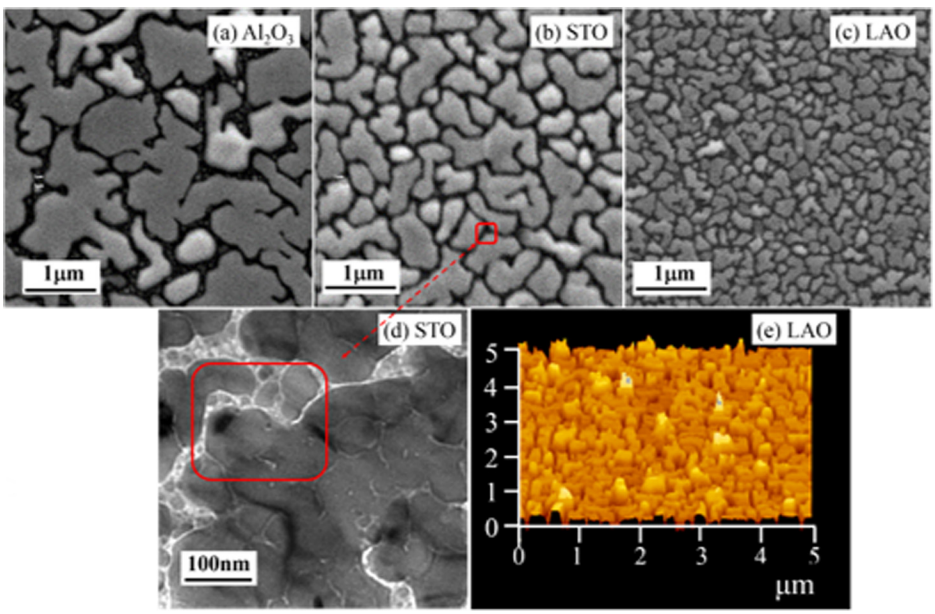

FIG. 1. SEM morphology of the 45 nm thin films on Al_2O_3 (a) STO (b), and LAO (c), the TEM images of a part of one island for the film grown on STO (d), and three dimensional AFM image of the film on LAO (e). The black vacancies in the SEM image (b) correspond to the white areas in the TEM image. The selected area in the TEM image corresponds to the selected island area in (b).

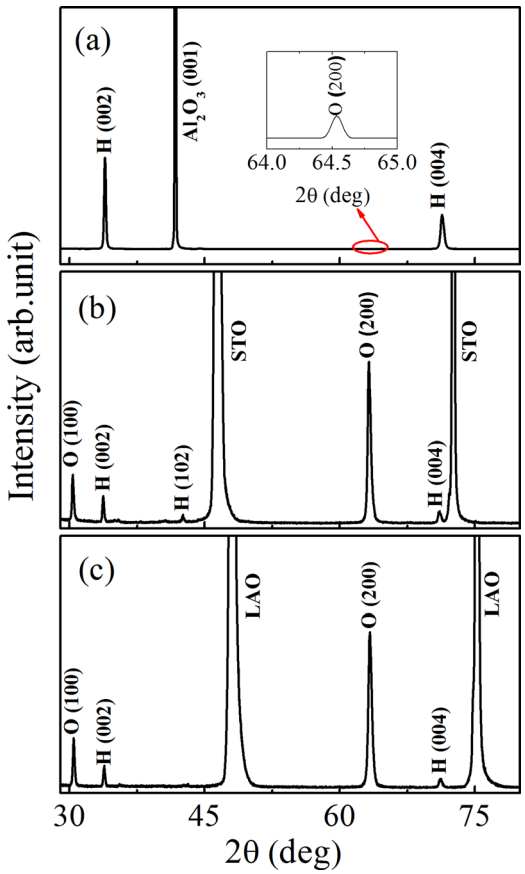

FIG. 2. XRD pattern of the Mn-Co-Ge-In films deposited on the (001)-cut Al_2O_3 (a), STO (b), and LAO (c) substrates, where "O" represents the orthorhombic structure and "H" represents the hexagonal structure of the Mn-Co-Ge-In alloy. The inset in (a) shows the enlarged image of the selected area.

out of plane, along which the lattice deformation is allowed and the reconstruction of the structure during the martensitic transition would be facilitated. The sketch of both structures and detailed analysis about film structure growth on different substrates can be found in the supplementary material.

The magnetic transformation behavior was determined by measuring the magnetization dependence on temperature (M-T curves). Both zero field cooling (ZFC) and field cooling (FC) modes were adopted with a magnetic field of 0.05 T applied (Fig. 3). For all the films deposited on different substrates, there exists an obvious thermal hysteresis in a wide temperature range, denoting the overlap of magnetic and structural transitions and the emergence of first order magnetostructural transformation (M_s).[2] The transformation window of the films is much more broadened when compared to that of the bulk alloy, which has a rapid transition at around 324 K with a thermal hysteresis of 6 K [Fig. 3(d)]. Differential M-T curves (dM/dT) on heating denote the minimum value at about 257 K for all the films, indicating that the magnetostructural transformation not only broadens but also shifts to lower temperature compared to the bulk. Still, there exists a dependence of M_s transformation behavior on the average island size of different films, that is, the M_s transformation is sharper for the film on Al_2O_3 with the largest average size but slower for the film on LAO with the smallest one.

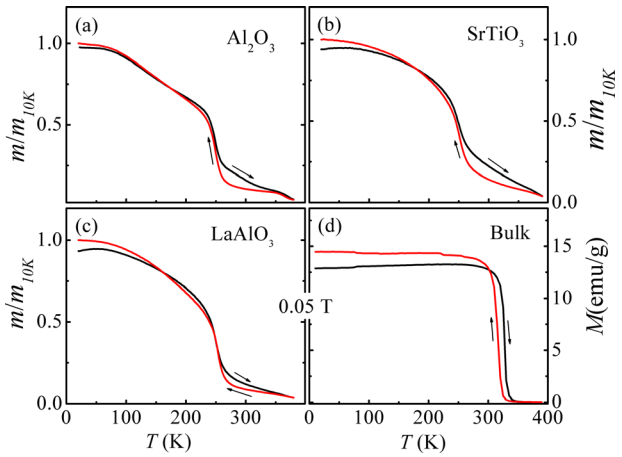

FIG. 3. The dependence of reduced magnetization on temperature (M-T curves) for the films grown on different substrates Al_2O_3 (a), STO (b), LAO (c), and M-T curves of the bulk alloy (d), with a magnetic field of 0.05 T applied. The arrows act as guides for the heating and cooling process, and red and black lines denote the FC and ZFC modes, respectively.

The M_s transformation of the MM'X family is very sensitive to the chemical components and external field such as hydrostatic pressure.[10] Moreover, size effect and residual stress could also influence its martensitic transformation.[29] Our previous studies[29] have demonstrated that with the reducing particle size, the austenite phase was stabilized and the transition window broadened in the hexagonal Mn-Ni-Fe-Ge alloy. The residual stress introduced in the cold pressed Mn-Co-Ge-In thin slice can be able to broaden the M_s transformation as well.[9] Furthermore, for the alloy films adhered to the substrates, the expansion of the film would certainly be constrained by the substrate. So it is conspicuous that for systems undergoing M_s, the transition will be inevitably influenced by the rigid substrate in the thin film system. One of the main sources of the stress in the thin films could be the crystal mismatch between the thin film and substrates. Furthermore, the thin films here have an island size much smaller than their bulk alloy and differ with each other. There would certainly exist crystal defects and surface stress which could vary with the island size. In the material with a fine-scale microstructure, the stresses from grain boundaries may give rise to internal stress fields that depend on the geometry. Thus, the different M_s transformation behavior of the films on different substrates can be closely related to the stress induced by the crystal mismatch and various grain sizes and residual stresses. Similar to the particle size effect reported in the Mn-Ni-Fe-Ge alloy,[29] the smallest island appears in the film on LAO, which corresponds to the slowest phase transition, compared to others on STO and Al_2O_3 (Fig. 3). It also predicts low thermal expansion behavior through the transformation.

As a representative display, Fig. 4 demonstrates the isothermal magnetization (M-H) curves for the film on STO substrate. The loops were measured with the applied magnetic field along the in-plane direction. All plots have been corrected to eliminate the influence from the diamagnetism of the substrate using the relationship: $M_{film} = M_{tota} - \chi H$, in which χ is the susceptibility of the substrate and H is the magnetic field applied. For a material with first order

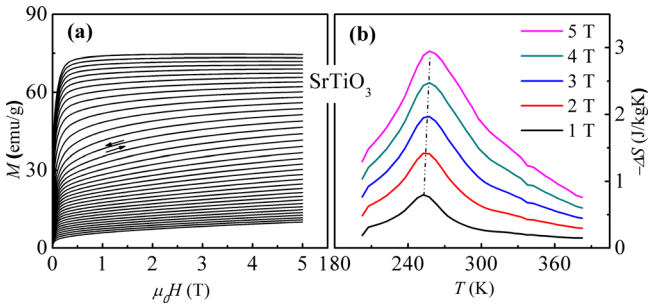

FIG. 4. The isothermal magnetization (M-H) curves (a) and the magnetic entropy change dependence on temperature under different magnetic fields (b) for the typical thin film grown on the STO substrate.

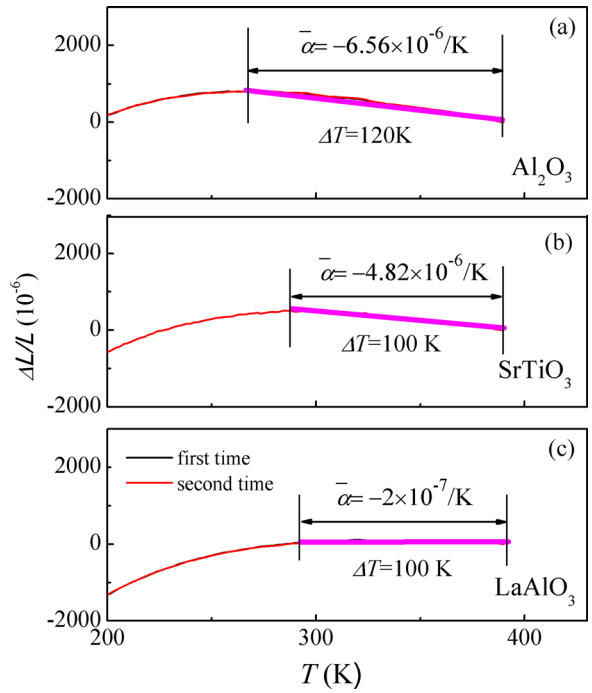

FIG. 5. Temperature dependence of linear thermal expansion $\Delta L/L$ for the different Mn-Co-Ge-In thin films grown on Al_2O_3 (a), STO (b), and LAO (c). Each has been repeated at least two times.

transition that lasts in a wide temperature window (not at a point), it has been proved that the Maxwell relation and Clausius-Clapeyron relations are the equal ways to calculate the isothermal entropy change.[30] Combined with the Maxwell relationship, the magnetic entropy change ΔS was calculated and is shown in Fig. 4(b). Approximately, the maximum $|\Delta S|$ values for magnetic field changes (ΔB) of 0–2 T and 0–5 T are about 1.4 and 3.0 J/kgK, and the temperatures corresponding to the $|\Delta S|$ maximum are 253 K and 258 K, respectively. In particular, $|\Delta S|$ under 2 T (the permanent magnet can reach) is comparable to the value reported in the well-known metamagnetic Ni-Co-Mn-In (1.1 J/kgK for $\Delta B = 2$ T)[23] and Ni-Mn-Sn (1.5 J/kgK for $\Delta B = 1$ T) thin films.[24] The $|\Delta S|$ value, which is intimately related to the M_s transformation, reasonably reduces compared to the giant MCE of its bulk which undergoes a sharp M_s. There is no obvious magnetic hysteresis in the M-H curves for the film, and the temperature span of half width of the ΔS peak is as wide as 100 K [Fig. 4(b)], originating from the broadened M_s transformation. Besides, refrigerant capacity (*RC*) is another parameter that could assess the MCE of a refrigerant. It reflects the energy that a refrigerant can transfer between the cold and hot sources. *RC* is defined as $RC = \int_{T_1}^{T_2} |\Delta S_M| dT$, where T_1 and T_2 are the temperatures corresponding to the half maximum of the ΔS peak. The RC values estimated for the film are 39 J/kg and 253 J/kg for $\Delta B = 2$ T and 5 T, respectively, which are higher than its bulk parent (189 J/kg for $\Delta B = 5$ T)[10] and the reported Ni-Mn-Sn thin films (33.9 J/kg for $\Delta B = 2$ T).[24] These results indicate potential applications of the present films for micro-scale magnetic cooling.

Moreover, we also studied the NTE behavior involving the magnetostructural transformation for the films. The thermal expansion coefficient α was determined using a high resolution strain gauge directly adhered onto the film surface. As can be seen from Fig. 5, the thin films denote NTE behavior, and multiple measurements demonstrate that the NTE behavior is completely repeatable without any fatigue. Moreover, we surprisingly found that the NTE coefficient α shows a monotonous decrease with the reducing island size (Fig. 1). For the films on Al_2O_3 and STO, the average island sizes are about 1 μm and 0.66 μm, and the NTE coefficients are $\alpha \sim -6.56 \times 10^{-6}$/K (from 270 K to 390 K) and $\alpha \sim -4.82 \times 10^{-6}$/K (from 290 K to 390 K), respectively. These α values are a bit smaller compared to those of the representative NTE materials ZrW_2O_8 ($\alpha \sim -9 \times 10^{-6}$/K).[11] For the film on LAO, the average island size (0.28 μm) becomes further smaller (Fig. 1), and the NTE coefficient further reduces and approaches zero ($\alpha \sim -2 \times 10^{-7}$/K) in a wide temperature range of 290 K to 390 K at around room temperature. More excitingly, the NTE behavior of all the films remains nearly independent of temperature in the corresponding temperature window, which is guided by the purple lines in Fig. 5. These characteristics are appreciable for practical application. The obvious dependence of NTE coefficient on the average island size of the alloy films should be intimately correlated with the variety of introduced residual strains and their impact on the first order magnetostructural transition process.[3] As discussed in the former part, the grain size of the alloy films is much smaller than the bulk reported,[29] which means that more grain boundaries and crystallite defects may appear. The surface stress and residual strain differ with the geometry, leading to the variation of the transformation temperature between different islands and hence the broadening of the phase transition window and the gradual reduction of NTE coefficient α with the reducing particle size.[3,31] Besides, the compensating effect from the positive thermal expansion of substrates as well as the possible stress introduced by the mismatch of different thermal expansions between the film and substrates[32,33] should also play an important role in the reduced NTE of films. Note that the linear thermal expansion coefficients of the commercially supplied Al_2O_3, STO, and LAO substrates are about $\alpha \sim +7.5 \times 10^{-6}$/K, $\alpha \sim +9.4 \times 10^{-6}$/K, and $\alpha \sim +1 \times 10^{-5}$/K, respectively. As the observed NTE here is a result upon compensating from the substrate, the temperature range and the NTE coefficient behave differently. This is a complex physical process, which is also closely related to the spreading of strains between the substrates and films, size effect, and possible defects.

The different strain state of the films, depending on the average island size, along with the thermal compensating effect from substrates, governs the NTE coefficient of the Mn-Co-Ge-In films. As the NTE material owns a lot of potential applications in the areas of machinery parts, optical fiber reflective gating devices, and printed circuit boards, it can act as compensators for positive thermal expansion materials to form composites with a precise thermal expansion coefficient. The approximately linear NTE of the film here is thus intriguing, based on which thin films with different coefficients of thermal expansion can be designed and grown through choosing appropriate substrates or introducing a buffer layer. Furthermore, the NTE behavior in present films is completely repeatable between different cycles and much more durable, which gives the films great advantage in practical applications.

See supplementary material for the sketch of orthorhombic and hexagonal structures and the detailed analysis on the film structure and growth on different substrates.

This work was supported by the National Key Research and Development Program of China (Grant Nos. 2017YFB0702702, 2014CB643700, and 2017YFA0303601), the National Natural Sciences Foundation of China (Grant Nos. 51531008, 51771223, 51590880, 11674378, and 11474341), and the Key Program and Strategic Priority Research Program (B) of the Chinese Academy of Sciences.

[1]E. K. Liu, W. H. Wang, L. Feng, W. Zhu, G. J. Li, J. L. Chen, H. W. Zhang, G. H. Wu, C. B. Jiang, H. B. Xu, and F. Boer, Nat. Commun. **3**, 873 (2012).
[2]R. R. Wu, L. F. Bao, F. X. Hu, H. Wu, Q. Z. Huang, J. Wang, X. L. Dong, G. N. Li, J. R. Sun, F. R. Shen, T. Y. Zhao, X. Q. Zheng, L. C. Wang, Y. Liu, W. L. Zuo, Y. Y. Zhao, M. Ming, C. X. Wang, C. Q. Chang, H. G. Rao, X. F. Han, and B. G. Shen, Sci. Rep. **5**, 18027 (2015).
[3]Y. Y. Zhao, F. X. Hu, L. F. Bao, J. Wang, H. Wu, Q. Z. Huang, R. R. Wu, Y. Liu, F. R. Shen, H. Kuang, M. Zhang, W. L. Zuo, X. Q. Zheng, J. R. Sun, and B. G. Shen, J. Am. Chem. Soc. **137**, 1746 (2015).
[4]K. Koyama, M. Sakai, T. Kanomata, and K. Watanabe, Jpn. J. Appl. Phys., Part 1 **43**, 8036 (2004).
[5]V. Johnson, Inorg. Chem. **14**, 1117 (1975).
[6]C. F. Sanchez-Valdes, J. L. Sanchez Llamazares, H. Flores-Zyniga, D. Rios-Jara, P. Alvarez-Alonso, and P. Gorria, Scr. Mater. **69**, 211 (2013).
[7]N. T. Trung, L. Zhang, L. Caron, K. H. J. Buschow, and E. Brück, Appl. Phys. Lett. **96**, 172504 (2010).
[8]E. K. Liu, W. Zhu, L. Feng, J. L. Chen, W. H. Wang, G. H. Wu, H. Y. Liu, F. B. Meng, H. Z. Luo, and Y. X. Li, Eur. Phys. Lett. **91**, 17003 (2010).
[9]N. T. Trung, V. Biharie, L. Zhang, L. Caron, and K. H. J. Buschow, Appl. Phys. Lett. **96**, 162507 (2010).
[10]Y. Liu, F. R. Shen, M. Zhang, L. F. Bao, R. R. Wu, Y. Y. Zhao, F. X. Hu, J. Wang, W. L. Zuo, J. R. Sun, and B. G. Shen, J. Alloys Compd. **649**, 1048 (2015).
[11]L. Caron, N. T. Trung, and E. Brück, Phys. Rev. B **84**, 020414(R) (2011).
[12]T. A. Mary, J. S. O. Evans, T. Vogt, and A. W. Sleight, Science **272**, 90 (1996).
[13]X. G. Zheng, H. Kubozono, H. Yamada, K. Kato, Y. Ishiwata, and C. N. Xu, Nat. Nanotechnol. **3**, 724 (2008).
[14]J. Chen, K. Nittala, J. S. Forrester, J. L. Jones, J. Deng, R. Yu, and X. R. Xing, Am. Chem. Soc. **133**, 11114 (2011).
[15]S. Iikubo, K. Kodama, K. Takenaka, H. Takagi, M. Takigawa, and S. Shamoto, Phys. Rev. Lett. **101**, 205901 (2008).
[16]Y. Sun, C. Wang, Q. Huang, Y. Guo, L. Chu, M. Arai, and K. Yamaura, Inorg. Chem. **51**, 7232 (2012).
[17]R. J. Huang, Y. Y. Liu, W. Fan, T. Tan, F. R. Xiao, H. L. Qian, and L. F. Li, Am. Chem. Soc. **135**, 11469 (2013).
[18]D. C. Dunand and P. Müllner, Adv. Mater. **23**, 216 (2011).
[19]C. W. Miller, D. V. Williams, N. S. Bingham, and H. Srikanth, J. Appl. Phys. **107**, 09A903 (2010).
[20]A. L. Pires, J. H. Belo, I. T. Gomes, R. L. Hadimani, D. C. Jiles, L. Fernandes, P. B. Tavares, J. P. Araújo, A. M. L. Lopes, and A. M. Pereira, Mater. Lett. **159**, 301 (2015).
[21]R. L. Hadimani, J. H. B. Silva, A. M. Pereira, D. L. Schlagel, T. A. Lograsso, Y. Ren, X. Y. Zhang, D. C. Jiles, and J. P. Araújo, Appl. Phys. Lett. **106**, 032402 (2015).
[22]T. J. Zhou, M. K. Cher, L. Shen, J. F. Hu, and Z. M. Yuan, Phys. Lett. A **377**, 3052 (2013).
[23]H. S. Akkera, I. Singh, and D. Kaur, J. Alloys Compd. **642**, 53 (2015).
[24]R. Niemann, O. Heczko, L. Schultz, and S. Fähler, Appl. Phys. Lett. **97**, 222507 (2010).
[25]E. Yuzuak, I. Dincer, Y. Elerman, A. Auge, N. Teichert, and A. Hutten, Appl. Phys. Lett. **103**, 222403 (2013).
[26]D. H. Mosca, F. Vidal, and V. H. Etgens, Phys. Rev. Lett. **101**, 125503 (2008).
[27]C. T. Campbell, Surf. Sci. Rep. **27**, 1 (1997).
[28]S. Kaprzyk and S. Niziol, J. Magn. Magn. Mater. **87**, 267 (1990).
[29]R. R. Wu, F. R. Shen, F. X. Hu, J. Wang, L. F. Bao, L. Zhang, Y. Liu, Y. Y. Zhao, F. X. Liang, W. L. Zuo, J. R. Sun, and B. G. Shen, Sci. Rep. **6**, 20993 (2016).
[30]J. R. Sun, F. X. Hu, and B. G. Shen, Phys. Rev. Lett. **85**, 4191 (2000).
[31]F. R. Shen, H. Kuang, F. X. Hu, H. Wu, Q. Z. Huang, F. X. Liang, K. M. Qiao, J. Li, J. Wang, Y. Liu, L. Zhang, M. He, Y. Zhang, W. L. Zuo, J. R. Sun, and B. G. Shen, APL Mater. **5**, 106102 (2017).
[32]I. R. Aseguinolaza, I. Orue, A. V. Svalov, K. Wilson, P. Müllner, J. M. Barandiarán, and V. A. Chernenko, Thin Solid Films. **558**, 449 (2014).
[33]I. R. Aseguinolaza, I. Reyes-Salazar, A. V. Svalov, K. Wilson, W. B. Knowlton, P. Müllner, J. M. Barandiarán, E. Villa, and V. A. Chernenko, Appl. Phys. Lett. **101**, 241912 (2012).